

Nuray Yıldız\*, Çağlar Ateş, Mehmet Yılmaz, Dürdane Demir, Atila Yıldız and Ayla Çalılı

# Investigation of lichen based green synthesis of silver nanoparticles with response surface methodology

**Abstract:** In this study, silver (Ag) nanoparticles were successfully biosynthesized from AgNO<sub>3</sub> through a simple green route using the lichen extract [*Cetraria islandica* (L) Ach] as a reducing and stabilizing agent. The mean sizes of spherical Ag nanoparticles with diameters ranging from 5 nm to 29 nm were obtained at different reaction conditions. The nanoparticles were characterized using transmission electron microscopy (TEM), energy dispersive X-ray (EDX), ultraviolet-visible (UV-VIS) and Fourier transform infrared spectroscopy (FTIR) techniques. Response surface methodology (RSM) was used to investigate the effects of temperature, reaction time and AgNO<sub>3</sub>/lichen ratio on green synthesis of Ag nanoparticles. The results showed that the increase in reaction time and AgNO<sub>3</sub>/lichen ratio caused a decrease of particle size and the increase in temperature resulted in bigger particles.

**Keywords:** biosynthesis; *Cetraria islandica* (L)Ach; characterization; lichen; RSM; silver nanoparticles.

DOI 10.1515/gps-2014-0024

Received March 20, 2014; accepted June 3, 2014; previously published online July 17, 2014

## 1 Introduction

In recent years, metal nanoparticles have taken attention, due to their superior electronic, catalytic, optical and magnetic properties [1]. Among the metal nanoparticles, silver (Ag) nanoparticles have attracted considerable attention

due to their wide applicability [2–5]. In addition to their antibacterial activity which has been known since ancient times [6], various attributes of Ag nanoparticles have been determined such as antifungal activity [7], antiinflammatory effects [8] antiviral activity [9] antiangiogenesis activity [10] and antiplatelet activity [11]. There is a variety of chemical and physical techniques to prepare metal nanoparticles, such as chemical reduction [12, 13], electrochemical reduction [14, 15], photochemical reduction [16, 17] and heat evaporation [18, 19]. Although there are different techniques to synthesize metallic nanoparticles, these methods have many disadvantages, for instance, the use of hazardous chemicals, high energy consumption and generation of hazardous by-products [20].

Nowadays, increasing awareness to develop environmentally benign methods has led to a desire to apply green chemistry techniques and other biological processes for the synthesis of nanoparticles. These processes have several advantages such as cost-effectiveness, simplicity, applicability to biomedical and pharmaceutical systems and reproducibility in a large scale [21].

There have been numerous reports in literature of synthesizing Ag nanoparticles via the biosynthesis route. Lately, plant and plant extracts [22, 23], yeast [23], fungi [24], bacteria [25] and mushrooms [26] have been used to obtain Ag nanoparticles for nontoxic production [27].

To the best of our knowledge, the use of lichen extract has not been investigated so far in the synthesis of Ag nanoparticles. Lichens are symbiotic associations consisting of a fungus and one or several algal or cyanobacterial components [28]. *Cetraria islandica* (L)Ach is a lichen species which has been used through the ages in folk medicine in many countries. It was reputed to be effective in treatment of pulmonary tuberculosis, throat irritation, gastritis, dry cough, diabetes, hemorrhoids, bronchitis and dysentery. Neither toxic effects nor drug interactions were reported with the use of *C. islandica*. *C. islandica* contains high proportions of polysaccharides (lichenan and isolichenan) and several secondary metabolites (such as protolichesterinic acid and fumarprotocetraric acid) [29, 30]. Bearing in mind the role of polysaccharides in the synthesis of nanoparticles, we intended to develop a

\*Corresponding author: Nuray Yıldız, Department of Chemical Engineering, Ankara University, 06100, Tandoğan, Ankara, Turkey, e-mail: nyildiz@eng.ankara.edu.tr

Çağlar Ateş, Dürdane Demir and Ayla Çalılı: Department of Chemical Engineering, Ankara University, 06100, Tandoğan, Ankara, Turkey

Mehmet Yılmaz: Department of Chemical Engineering Division of Bioengineering, Hacettepe University, 06800, Beytepe, Ankara, Turkey

Atila Yıldız: Department of Biology, Ankara University, 06100, Tandoğan, Ankara, Turkey

green synthesis route to obtain Ag nanoparticles using *C. islandica* as a reducing agent.

Although there are many studies in literature, controllable green synthesis of Ag nanoparticles is still a major challenge that should be eliminated. Response surface methodology (RSM) is a reliable method to examine controllable biosynthesis of Ag nanoparticles. In this study, it is the first time to investigate green synthesis of Ag nanoparticles using the extract of *C. islandica* via RSM. RSM design was applied to determine the effects of temperature, reaction time and AgNO<sub>3</sub>/lichen ratio (ml/ml) on controllable green synthesis of Ag nanoparticles. Synthesized nanoparticles were characterized by transmission electron microscopy (TEM), energy dispersive X-ray (EDX), ultraviolet-visible (UV-VIS) and Fourier transform infrared spectroscopy (FTIR) analyses.

## 2 Materials and methods

### 2.1 Materials

The lichen (*C. islandica*) was collected from the middle Anatolian region of Turkey (Yapraklı, Çankırı). Silver nitrate (AgNO<sub>3</sub>) was purchased from Sigma-Aldrich Chemicals. Aqueous AgNO<sub>3</sub> solution (10 mM) was prepared using double distilled water.

### 2.2 Extraction of *C. islandica*

The lichen was washed with copious quantities of deionized water and cleaned under an optical microscope to remove surface impurities and extraneous materials. Lichen samples were ground to a fine powder for extraction. Powdered lichen material was extracted by Soxhlet extraction with ethanol and the extract was filtered and stored at 4°C for further experiments.

### 2.3 Synthesis of Ag nanoparticles by *C. islandica* extract

In a typical reaction procedure, the proper amount of lichen extract was added to 10 mM aqueous AgNO<sub>3</sub> solution. The mixture was stirred in a shaking incubator (Zhicheng ZHWY-200B, China) at constant rate (350 rpm). The resulting solution became pale yellow in color.

## 2.4 Characterization of Ag nanoparticles

UV-VIS spectroscopic studies of synthesized Ag nanoparticles were carried out using a Shimadzu-UV 1601 (Japan) spectrophotometer in a range between 300 nm and 900 nm. The morphology and size distribution of Ag nanoparticles were analyzed by TEM (FEI Tecnai Gz F30, USA) with EDX. In order to determine the functional groups on the dried lichen extract and their possible involvement in the synthesis of Ag nanoparticles, FTIR analysis was carried out with a Shimadzu 8400 S FTIR (Japan) spectrophotometer in a range of 450–2000 cm<sup>-1</sup>. The FTIR spectra of *C. islandica* extract were taken before and after the synthesis of Ag nanoparticles.

## 2.5 Experimental design with RSM

RSM consisting of a group of empirical techniques was used in the present report. The method was devoted to the evaluation of relations between controlled experimental parameters and the measured responses according to one or more criteria [31]. An experimental design such as the central composite design (CCD) to fit a model by the least squares technique was used in RSM. If the proposed model is suitable, as revealed by the diagnostic checking provided by an analysis of variance (ANOVA), contour plots can be usefully exploited to study the response and locate the optimum.

The previous studies showed that the temperature, reaction time and AgNO<sub>3</sub>/lichen extract agent ratio are important parameters for synthesis of Ag nanoparticles. The effects of these variables on synthesis of Ag nanoparticles were studied using RSM. The most common experimental design used in RSM is the CCD, which has equal predictability in all directions from the center. According to the CCD, the total number of combinations is  $2k+2k+n_0$ , where  $k$  is the number of independent variables and  $n_0$  is the number of repetitions of the experiments at the center point [32].

The range and the levels of the variables investigated in this study are shown in Table 1. On the basis of

**Table 1** Coded value of the independent variables and experimental ranges.

Independent variables	Range and levels				
	-1.68	-1	0	1	1.68
Time, min ( $x_1$ )	19.09	60	120	180	220.91
AgNO <sub>3</sub> /lichen ratio (ml/ml) ( $x_2$ )	0.31	1.5	3.25	5	6.19
Temperature (°C), ( $x_3$ )	16.48	25	37.5	50	58.52

preliminary experiments, the range of temperature, reaction time and  $\text{AgNO}_3$ /lichen extract ratio were chosen as 25–50°C, 60–180 min and 1.5–5 (ml/ml), respectively.

The test variables, in the model equation were coded according to the equation (1):

$$x_i = \frac{X_i - X_i^*}{\Delta X_i} \quad (1)$$

where  $x_i$  is the coded value of the  $i$  th independent variable,  $X_i$  is the uncoded value of the  $i$  th independent variable,  $X_i^*$  is the uncoded value of the  $i$  th independent variable at the center point and  $\Delta X_i$  is the step change value. The response of the system was expressed by the following second degree polynomial equation [32]:

$$Y = B_0 + \sum_{i=1}^n B_i x_i + \sum_{ij} B_{ij} x_i x_j + \sum_{j=1}^n B_{jj} x_j^2 \quad (2)$$

where  $Y$  is the predicted response, three variables are involved and hence  $n$  takes 3 in this study. Thus by substituting the value 3 for  $n$ , Eq. (2) becomes:

$$Y = B_0 + B_1 x_1 + B_2 x_2 + B_3 x_3 + B_{12} x_1 x_2 + B_{13} x_1 x_3 + B_{23} x_2 x_3 + B_{11} x_1^2 + B_{22} x_2^2 + B_{33} x_3^2 + \varepsilon \quad (3)$$

where  $x_1$ ,  $x_2$  and  $x_3$  are input variables;  $B_0$  is a constant;  $B_1$  and  $B_2$  are linear coefficients;  $B_{12}$  is the interaction

coefficient,  $B_{11}$  and  $B_{22}$  are quadratic coefficients and  $\varepsilon$  is experimental error.

In this study,  $2^3$  full factorial CCD for three independent variables each at five levels with six axial points (with an axial distance of  $\pm 1.68$  for making this design orthogonal) and six replicate at the center points was employed to fit a second order polynomial model which indicated that 20 experiments were required for this procedure (Table 2). The size of Ag nanoparticles was chosen as the response variable measured by TEM analysis.

The “Design Expert” software (version 6.06, Stat-Ease Inc., Minneapolis, MN, USA) was employed for regression and plotting of the data obtained. The fit of the regression model was checked by the adjusted coefficient of determination ( $R_{adj}^2$ ). The statistical significance of the model was determined by the application of Fisher’s F test.

### 3 Results and discussion

To confirm the formation of Ag nanoparticles by lichen extract, UV-VIS spectral analyses were performed. The effects of reaction time, temperature and  $\text{AgNO}_3$ /lichen ratio on Ag nanoparticles are shown in Figure 1. The characteristic surface plasmon absorption bands are observed between 405 and 438 nm. This observation indicates the formation of nanometer sized Ag nanoparticles in all runs.

**Table 2** Experimental design for coded and real values with related response (mean particle size).

Exp. run	$x_1$	$x_2$	$x_3$	Time (min)	$\text{AgNO}_3$ /lichen ratio (ml/ml)	Temperature (°C)	Mean particle size (nm) (response)
1	-1	1	1	60	5.00	50.00	18.4
2	1.68	0	0	220.91	3.25	37.50	9.5
3	1	1	-1	180	5.00	25.00	9.9
4	0	0	0	120	3.25	37.50	6.6
5	-1	1	-1	60	5.00	25.00	11.5
6	0	0	0	120	3.25	37.50	6.6
7	1	-1	1	180	1.50	50.00	5.6
8	-1.68	0	0	19.09	3.25	37.50	21.8
9	-1	-1	-1	60	1.50	25.00	6.9
10	0	0	1.68	120	3.25	58.52	6.9
11	0	0	0	120	3.25	37.50	6.1
12	0	0	0	120	3.25	37.50	7.1
13	0	-1.68	0	120	0.31	37.50	9
14	0	0	0	120	3.25	37.50	6.7
15	0	1.68	0	120	6.19	37.50	28.6
16	1	-1	-1	180	1.50	25.00	10
17	0	0	0	120	3.25	37.50	6.6
18	1	1	1	180	5.00	50.00	12.9
19	-1	-1	1	60	1.50	50.00	8.6
20	0	0	-1.68	120	3.25	16.48	10.9

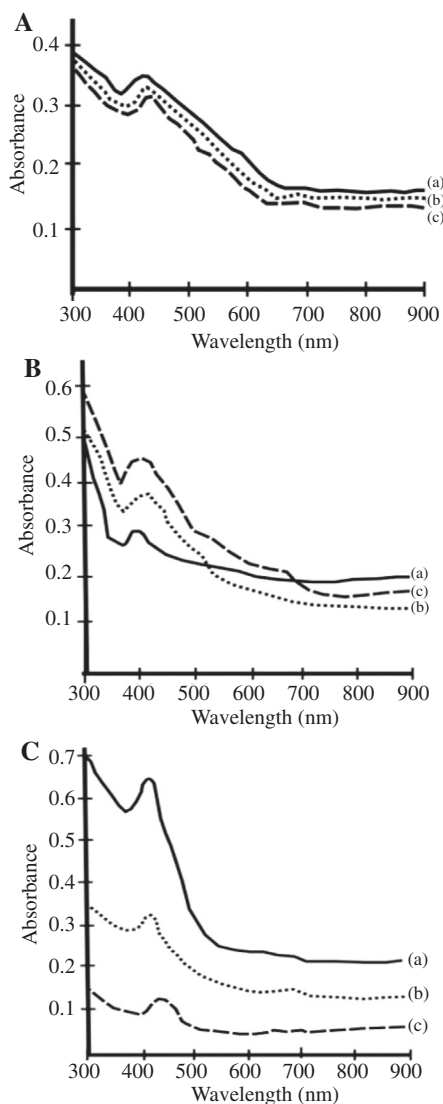


**Figure 1** UV-visible spectra of silver colloids. (A) The effect of reaction time at constant temperature (40°C) and AgNO<sub>3</sub>/lichen ratio (3.25) (a) 220 min, (b) 120 min and (c) 20 min. (B) The effect of reaction temperature at constant time (120 min) and AgNO<sub>3</sub>/lichen ratio (3.25) (a) 60°C, (b) 40°C and (c) 15°C. (C) The effect of AgNO<sub>3</sub>/lichen ratio at constant time (120 min) and temperature (40°C) (a) 0.31, (b) 3.25 and (c) 6.

The increase in the absorbance values with increasing reaction time (20–220 min) represents the higher production of Ag nanoparticles (Figure 1A). UV-VIS spectral measurement illustrates that the peak became sharper and the color of solution samples changed rapidly to pale yellow by increasing time. This result indicates the formation of Ag nanoparticles in a few minutes. The time needed to form Ag nanoparticles in our study was much lower than the earlier reports [33, 34]. Decrease in temperature and AgNO<sub>3</sub>/lichen ratio also resulted in increase of absorbance values (Figures 1B–1C). Increasing the

reaction temperature from 15°C to 60°C caused a decrease in the value of the surface plasmon resonance (SPR) band, depending on particle size distribution. Intensity of color and the SPR band maxima increased with increase in the lichen extract dosage (i.e., lower AgNO<sub>3</sub>/lichen ratio, see Figure 1C). The increase in the SPR band with decreasing AgNO<sub>3</sub>/lichen ratio represents the higher production of Ag nanoparticles, which is due to the availability of more reducing biomolecules for the reduction of Ag ions. The higher Ag nanoparticles' size is obtained at high AgNO<sub>3</sub>/lichen ratio due to the lack of biomolecules [35].

Figures 2–4 show representative TEM images and the corresponding size distribution histogram of Ag nanoparticles. The effects of reaction time at a constant temperature (40°C) and AgNO<sub>3</sub>/lichen ratio (3.25) are presented in Figures 2A–2C. From the size distribution histogram in Figure 2A, we could identify that the synthesized nanoparticles were distributed in a size range <15 nm. The histogram shows that there are variations in the particle sizes, with almost 50% of the particles in the 9 nm range, 27% in the 14 nm range and 15% in the 4 nm range; there were small percentages in the long range diameters of 2, 3, 7, 8, 11 and 18 nm. Furthermore, the variation of size is possibly due to the fact that the nanoparticles are formed at different times. Figure 2B shows two notable size distributions of particles, one having diameters in the range 1–7 nm and the others in the range 7–14 nm. Two broad size distributions of particles are also obtained in Figure 2C, one having diameters in the range 1–10 nm and the other with some larger diameters in the range 10–60 nm. The TEM images and histograms showing the effect of reaction temperature on the nanoparticle size are given in Figures 3A–3C. As the reaction temperature increases from 15°C to 60°C, the nanoparticles' sizes varies between 2 nm and 23 nm, 1 nm and 14 nm and 1 nm and 17 nm, respectively, and the average particle size decreases from 10.9 nm to 6.9 nm. The increase in reaction temperature results in a higher reaction rate and lower particle size as stated earlier. The TEM images and histograms in Figures 4A–4C show that the particle size increases with decrease in lichen extract dosage (i.e., higher AgNO<sub>3</sub>/lichen ratio). The results show that at the highest AgNO<sub>3</sub>/lichen ratio, two size distributions of particles are obtained, one with diameters in the range 1–15 nm and the other larger particles varying from 16 nm to 118 nm. The increase in particle size is due to a lack of enough reducing biomolecules for the reaction of Ag ions.

The EDX spectrum of run 12 (see Table 1) demonstrates the presence of Ag, Cu and some other elements due to the reduction of Ag ions in the presence of biomolecules (Figure 5). Herein, the signal of Cu is related to the



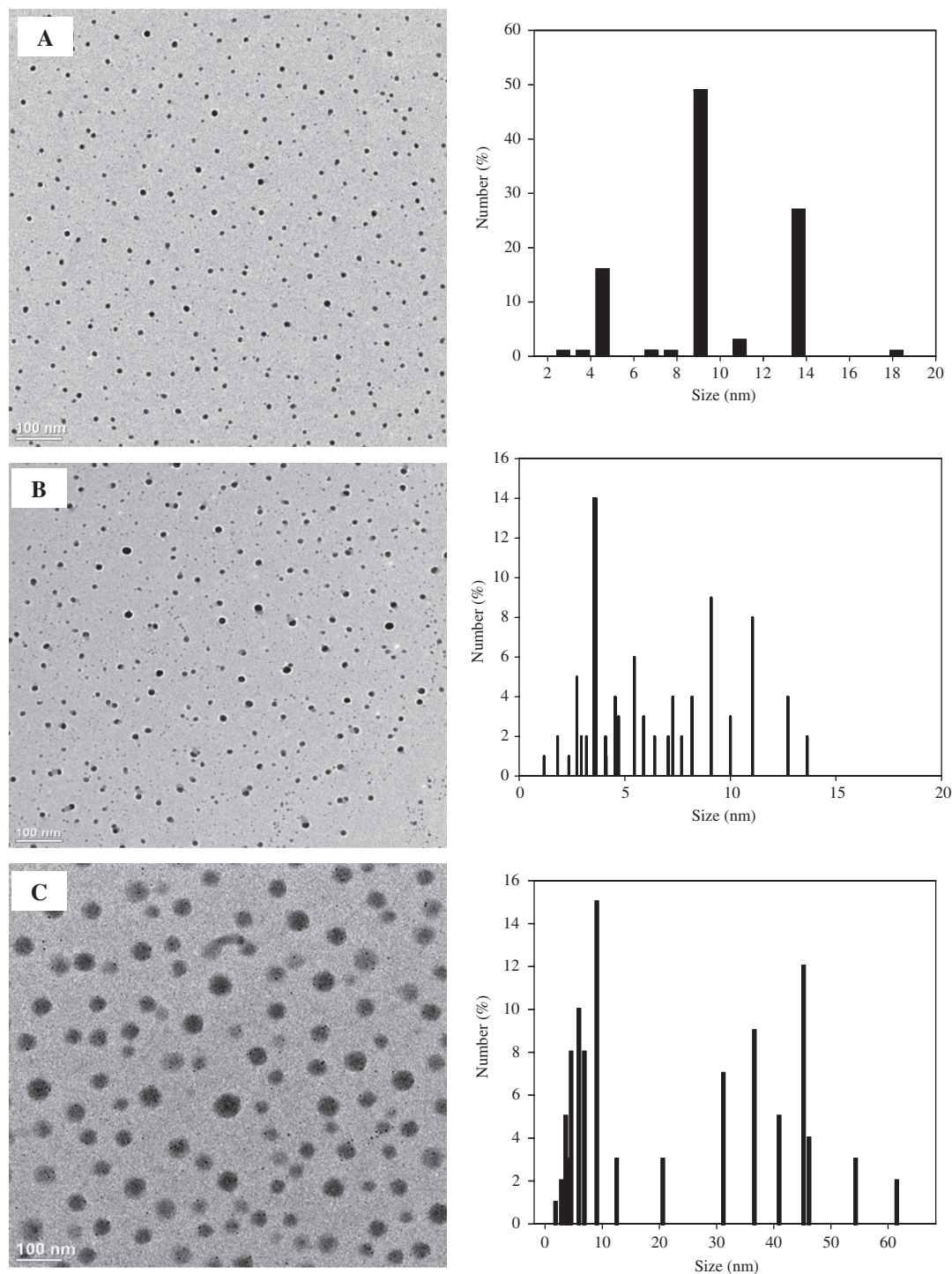


**Figure 2** Typical transmission electron microscopy (TEM) images and the corresponding size distribution histograms of synthesized Ag nanoparticles at constant temperature ( $40^{\circ}\text{C}$ ) and  $\text{AgNO}_3$ /lichen ratio (3.25): (A) 220 min, (B) 120 min and (C) 20 min.

background from the supporting copper grid. The optical absorption peak observed at approximately 3 keV confirms the presence of nanocrystalline elemental Ag [34].

FTIR analysis was carried out to identify the possible biomolecules account for the reduction of  $\text{Ag}^+$  ions and

efficient stabilization of Ag nanoparticles synthesized using lichen extract. FTIR spectra of dried lichen extract and Ag nanoparticles are shown in Figure 6. The FTIR spectral analysis revealed the presence of absorption peaks at  $1750\text{ cm}^{-1}$ ,  $1650\text{ cm}^{-1}$ ,  $1270\text{ cm}^{-1}$  and  $840\text{ cm}^{-1}$ . These

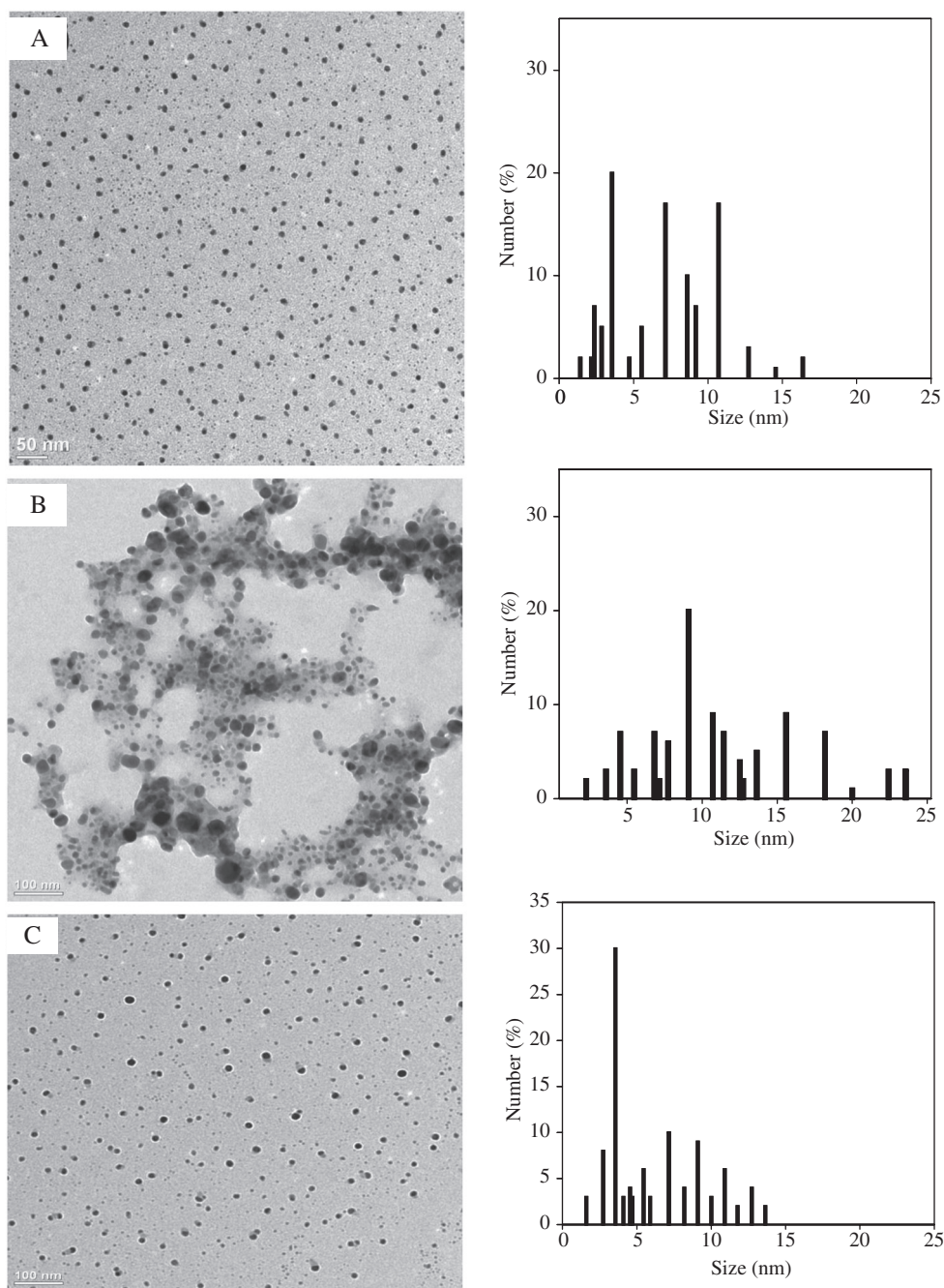


**Figure 3** Typical transmission electron microscopy (TEM) images and the corresponding size distribution histograms of synthesized Ag nanoparticles at constant reaction time (120 min) and  $\text{AgNO}_3$ /lichen ratio (3.25): (A) 60°C, (B) 15°C and (C) 40°C.

bands are attributed to alkene, ester, ether and aromatic structures in the lichen extract. The absorption band at  $1750\text{ cm}^{-1}$  is due to carbonyl stretching vibration of the acid groups of different fatty acids present in the lichen extract and the band at  $1650\text{ cm}^{-1}$  is the characteristic peak of amide [9]. Some other peaks at  $1270\text{ cm}^{-1}$  (C-O, C-N) and  $840\text{ cm}^{-1}$  (O-H) are also observed (Figure 6A). A comparison between the spectra of untreated samples to the treated samples of Ag nanoparticles revealed alterations

in the position as well as on the magnitude of the absorption bands (Figure 6A and 6B). After the bioreduction of  $\text{AgNO}_3$ , the shift of bands towards a lower frequency in the Ag nanoparticles indicates the efficient adsorption of lichen extract on the surface of the Ag nanoparticles and also the shift in the peak at  $1750\text{ cm}^{-1}$  towards a lower frequency is attributed to binding of  $-\text{C}=\text{O}$  group with nanoparticles (Figure 6B). Small shifts in band positions at  $1650\text{ cm}^{-1}$  and  $1270\text{ cm}^{-1}$  are assigned the electrostatic

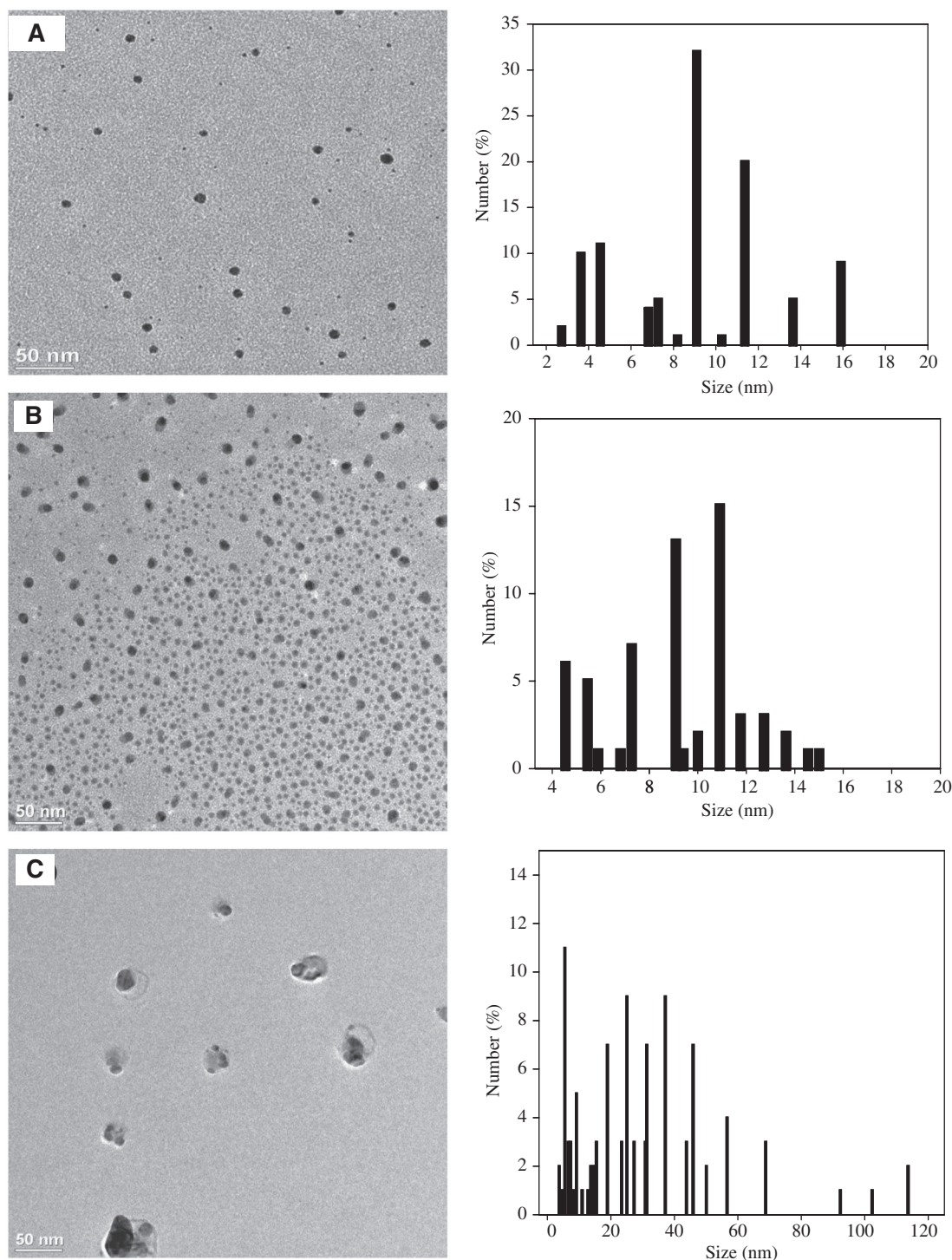


**Figure 4** Typical transmission electron microscopy (TEM) images and the corresponding size distribution histograms of synthesized Ag nanoparticles at constant reaction time (120 min) and temperature (40°C): (A) AgNO<sub>3</sub>/lichen: 0.30, (B) AgNO<sub>3</sub>/lichen: 3.25, (C) AgNO<sub>3</sub>/lichen: 6.

attractive forces between amino groups in polysaccharide and Ag<sup>+</sup> nanoparticles. Our FTIR findings collaborate with reports in the literature where polysaccharides are responsible for reduction and stabilization of Ag nanoparticles [36].

### 3.1 Experimental design with RSM

On the basis of preliminary experiments, the effects of AgNO<sub>3</sub>/lichen ratio, time and temperature on the size of Ag nanoparticles were studied with RSM. Average particle



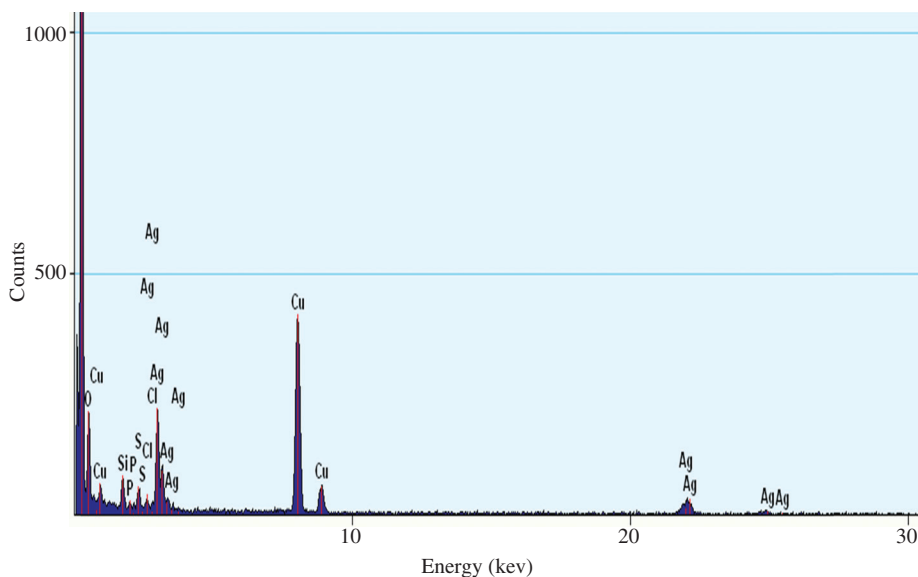


**Figure 5** Energy dispersive X-ray (EDX) spectrum (120 min, 3.25 AgNO<sub>3</sub>/lichen extract ratio, 60°C).

sizes represented in Table 2 are obtained from TEM images of each run by measuring much more than 100 particles. The application of RSM yields the following regression equation, which is an empirical relationship between the particle size of Ag nanoparticles and test variables in a coded unit. The second order polynomial equation for nanoparticle synthesis is as follows:

$$Y = 6.76 - 2.03x_1 + 4.00x_2 + 0.035x_3 + 2.25x_1^2 + 3.37x_2^2 - 0.13x_3^2 - 0.90x_1x_2 - 1.25x_1x_3 + 1.58x_2x_3 \quad (4)$$

where  $Y$  is the response, that is particle size of Ag nanoparticles and  $x_1$ ,  $x_2$  and  $x_3$  are coded terms for the test

variable, time, AgNO<sub>3</sub>/lichen ratio and temperature, respectively.

A summary of the ANOVA is given in Table 3. The ANOVA of quadratic regression model represents that the model is highly significant, as is evident by the Fisher's F-test value being 4.35, with a low probability value ( $P_{\text{model}} > F$ , 0.0156) lower than 0.05. Although the lack of a high F-value makes the model weaker, ANOVA results show that the reaction time and AgNO<sub>3</sub>/lichen ratio have a significant effect on the particle size. The goodness of the fit of the model is checked by determination of the regression constant ( $R^2$ ) value. In this model,  $R^2$  and the adjusted regression constant ( $R_{\text{adj}}^2$ ) are determined as 0.80 and 0.61, respectively. In the model, an adequate

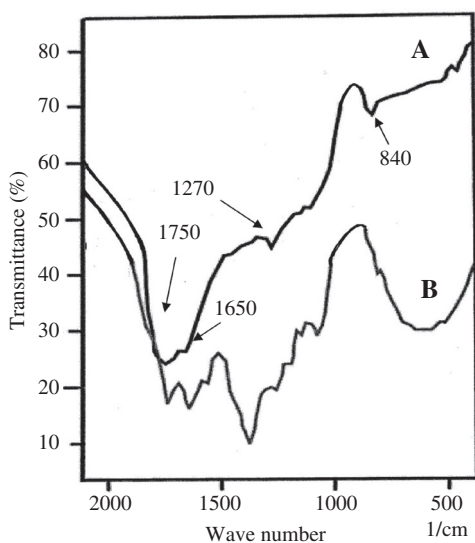


**Figure 6** Fourier transform infrared spectroscopy (FTIR) spectra of (A) dried lichen extract and (B) dried powder of silver nanoparticles.

**Table 3** ANOVA test results to determine accuracy of particle size model test.

	F	Prob>F
Model	4.35	0.0156
$x_1$	4.10	0.0704
$x_2$	15.93	0.0026
$x_3$	1.196E-003	0.9731
$x_1^2$	5.35	0.0432
$x_2^2$	11.95	0.0062
$x_3^2$	0.018	0.8951
$x_1x_2$	0.47	0.5071
$x_1x_3$	0.91	0.3618
$x_2x_3$	1.45	0.2563
Lack of fit test	268.26	<0.0001
Standard deviation		3.70
$R^2$		0.80
$R_{\text{adj}}^2$		0.61



precision value showing the ratio of response to deviation is found and required to be higher than 4. The obtained ratio of 7.136 indicates an adequate signal in the cause of optimization for Ag nanoparticles synthesis.

Corresponding  $p$  values suggest that, among the test variables used in this study,  $x_2$  ( $\text{AgNO}_3/\text{lichen}$  ratio),  $x_1$  (time),  $x_1^2$  (time)<sup>2</sup>,  $x_2^2$  ( $\text{AgNO}_3/\text{lichen}$  ratio)<sup>2</sup> are significant model terms with  $p$  values  $<0.05$ . Other interactions are found to be insignificant. The regression coefficient ( $R^2$ ) of the model is 0.80, which implies that the model adequately indicated the relationships among the selected parameters. The plots of three-dimensional response surfaces with one variable kept at constant level and the other two varying with the experimental ranges are given in Figures 7A–C. The nature of the counter plots represents that the mutual interaction between particle size and  $\text{AgNO}_3/\text{lichen}$  extract ratio and time is more than that between particle size and time or temperature. As can be seen, the mean size of Ag nanoparticles decreases by

increasing the reaction time and decreasing the  $\text{AgNO}_3/\text{lichen}$  extract ratio.

Similar findings were reported in literature. Dubey et al. [23] found that with an increase in levels extract quantity, the particle size of synthesized Ag nanoparticles decreased and Ag nanoparticles possessed more uniform shape. Janardhanan et al. [37] showed that increasing the  $\text{AgNO}_3$  concentration from 3 mM to 300 mM caused an increase of particle sizes from 40 nm to 630 nm, growing towards bulk Ag.

In literature, Ag nanoparticles with diameters ranging from 2 nm to 500 nm were obtained (Table 4) by different agents. These data show that lichen extract used as a reducing and stabilizing agent in this study has high efficiency for synthesizing Ag nanoparticles.

Experimental results clearly indicate that a highly safe and ecofriendly controllable green synthesis was developed for synthesis of Ag nanoparticles in aqueous lichen extract. Using different lichen extracts as reducing

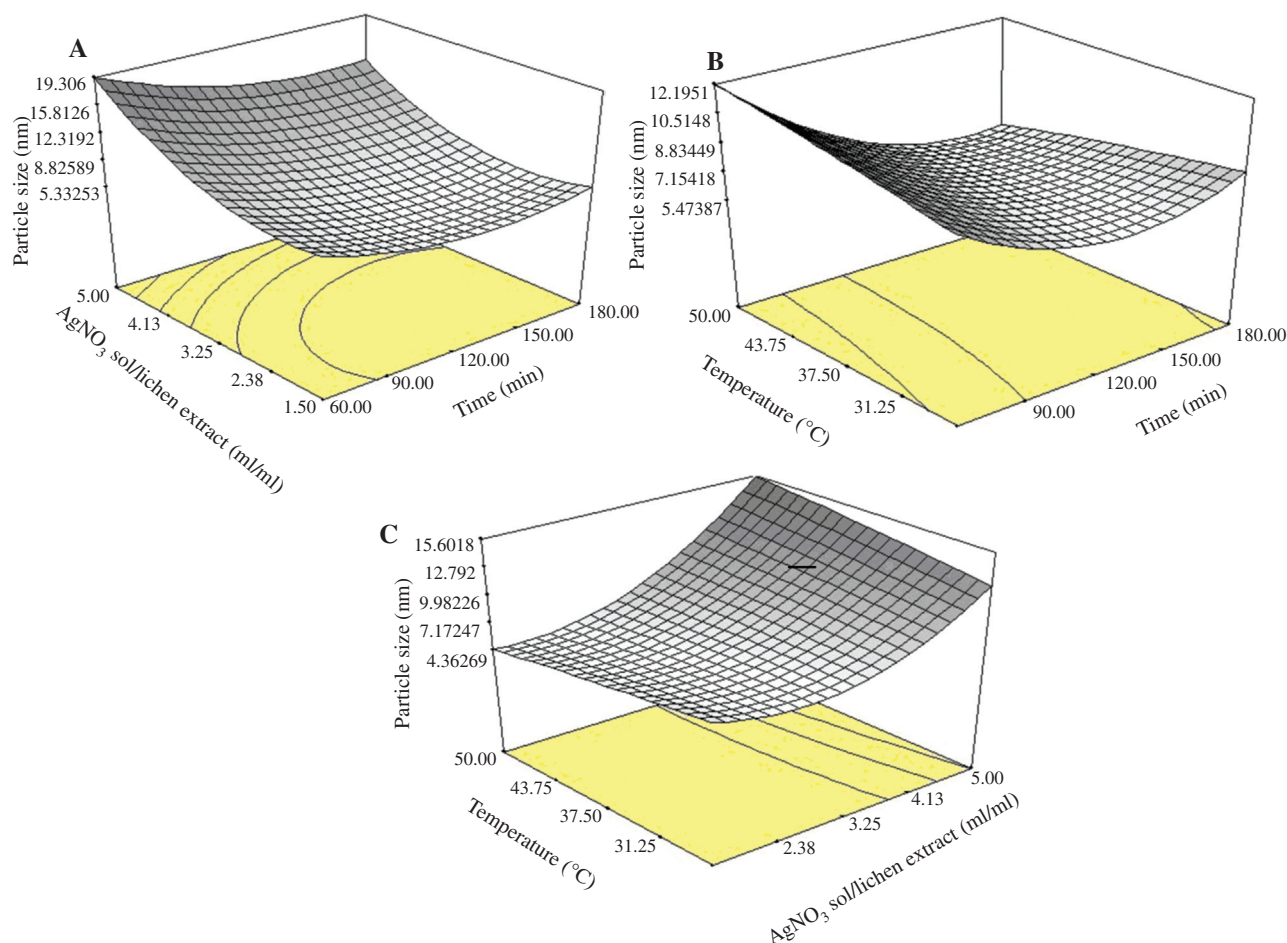


**Figure 7** Three-dimensional counter plots. (A) Particle size as a function of time and  $\text{AgNO}_3/\text{lichen}$  extract ratio at constant temperature (37.5°C), (B) as a function of time and temperature at constant  $\text{AgNO}_3/\text{lichen}$  extract ratio (3.25) and (C) as a function of temperature and  $\text{AgNO}_3/\text{lichen}$  extract ratio at constant time (120 min).

**Table 4** Synthesis of silver nanoparticles by different agents.

References	Nanoparticle size range (nm)	Stabilizing and reducing agent
Bar et al. [22]	10–20	Latex of <i>Jatropha curcas</i>
Bar et al. [2]	15–20	Seed extract of <i>Jatropha curcas</i>
Philip [26]	~15	Edible mushroom extract
Thakar et al. (review) [27]	2–500	Different bacteria, fungi, yeast, algae, plant and plant extracts
Kalishwaralal et al. [10]	10–50	<i>Brevibacterium casei</i>
Philip [38]	~4	Honey
Bankar et al. [39]	~300	Banana peel extract
Sathiyarayanan et al. [36]	~6	<i>Bacillus subtilis</i> (MSBF17)
Prakash et al. [40]	55–83	Leaf extract of <i>Mimusops elengi</i> , Linn.
Kumar et al. [41]	50–100	<i>Alternanthera dentata</i> leaf extract
Sun et al. [42]	20–90	Tea leaf extract
Dong et al. [43]	3–17	Hydroxy propyl methyl cellulose
In this study	5–29	Lichen extract [ <i>Cetraria islandica</i> (L)Ach]

agents, similar controllable studies can be conducted to synthesize various metal nanoparticles such as gold, platinum, palladium, copper, titanium, chrome, zinc etc. for various applications.

## 4 Conclusion

In the present work, Ag nanoparticles were synthesized by using lichen extract (*C. islandica* (L)Ach) as a reducing and stabilizing agent and the method applied was effective and truly a green approach. The statistically optimized medium was economically feasible for biosynthesis of Ag nanoparticles for commercial applications.

Apart from being environmentally benign, there is a key advantage of using lichen extract as a reducing agent. From the results obtained, it was found that the mean size of Ag nanoparticles with diameters ranging from 5 nm to 29 nm may be controlled by varying the AgNO<sub>3</sub>/lichen extract ratio, reaction time and temperature. Ag nanoparticle production using this process may be useful for biological applications, due to the biocompatibility of lichen extract.

**Acknowledgments:** This work was financially supported by Ankara University Scientific Research Project (Project No: 10Ö4343004).

## References

- [1] Ozin GA. *Adv. Mater.* 1992, 4, 612–649.
- [2] Bar H, Bhui DK, Sahoo GP, Sarkar P, Pyne S, Misra A. *Colloids Surf. A* 2009, 348, 212–216.
- [3] Mokhtari N, Daneshpajouh S, Seyedbagheri S, Atashdehghan R, Abdi K, Sarkar S, Minaian S, Shahverdi HR, Shahverdi AR. *Mater. Res. Bull.* 2009, 44, 1415–1421.
- [4] Lin JC, Wang CY. *Mater. Chem. Phys.* 1996, 45, 136–144.
- [5] Gould IR, Lenhard JR, Muentner AA, Godleski SA, Farid S. *J. Am. Chem. Soc.* 2000, 122, 11934–11943.
- [6] Bechert T, Steinrucke P, Wagener M, Seidel P, Dingeldein E, Domann E, Schnettler R. *Biomaterials* 2004, 25, 4383–4391.
- [7] Kim K, Sung W, Suh B, Moon S, Choi J, Kim J, Lee D. *Biometals* 2009, 22, 235–242.
- [8] Nadworny L, Wang J, Tredget EE, Burrell RE. *Nanomedicine* 2008, 4, 241–251.
- [9] Rogers JV, Parkinson CV, Choi YW, Speshock JL, Hussain SM. *Nanoscale Res. Lett.* 2008, 3, 129–133.
- [10] Kalishwaralal K, Banumathi E, Pandian SRK, Deepak V, Muniyandi J, Eom SH, Gurunathan S. *Colloids Surf. B* 2009, 73, 51–57.
- [11] Shrivastava S, Bera T, Singh SK, Singh G, Ramachandrarao P, Dash D. *ACS Nano* 2009, 3, 1357–1364.
- [12] Devaux X, Laurent Ch, Rousset A. *Nanostruct. Mater.* 1993, 2, 339–346.
- [13] Tan Y, Wang Y, Jiang L, Zhu D. *J. Colloids Interf. Sci.* 2002, 249, 336–345.
- [14] Liu YC, Lin LH. *Electrochem. Commun.* 2004, 6, 1163–1168.
- [15] Sandmann G, Dietz H, Plieth W. *J. Electroanal. Chem.* 2000, 491, 78–86.
- [16] Mallick K, Witcomb MJ, Scurrilla MS. *Mater. Chem. Phys.* 2005, 90, 221–224.
- [17] Keki S, Torok J, Deak G, Daraczi L, Zsuga M. *J. Colloids Interf. Sci.* 2000, 229, 550–553.
- [18] Bae CH, Nam SH, Park SM. *Appl. Surf. Sci.* 2002, 197, 628–634.
- [19] Smetana AB, Klabunde KJ, Sorensen CM. *J. Colloids Interf. Sci.* 2005, 284, 521–526.
- [20] Qi Z, Zhou H, Matsuda N, Honma I, Shimada K, Takatsu A, Kato K. *J. Phys. Chem. B* 2004, 108, 7006–7011.
- [21] Filippo E, Serra A, Buccolieri A, Mano D. *J. Non-Cryst. Solids* 2010, 356, 344–350.
- [22] Bar H, Bhui DK, Sahoo GP, Sarkar P, Sankar PD, Misra A. *Colloids Surf. A* 2009, 339, 134–139.
- [23] Dubey SP, Lahtinen M, Sillanpaa M. *Colloids Surf. A* 2010, 364, 34–41.

- [24] Chen JC, Lin ZH, Ma XX. *Lett. Appl. Microbiol.* 2003, 37, 105–108.
- [25] Klaus T, Joerger R, Olsson E, Granqvist CG. *Natl. Acad. Sci.* 1999, 96, 13611–13614.
- [26] Philip D. *Spectrochim. Acta, Part A* 2009, 73, 374–381.
- [27] Thakkar KN, Mhatre SS, Parikh RY. *Nanomed. Nanotechnol. Biol. Med.* 2010, 6, 257–262.
- [28] Yuan X, Xiao S, Taylor TN. *Science* 2005, 308, 1017–1020.
- [29] Olafsdottir ES, Ingólfssdottir K. *Planta Med.* 2001, 67, 199–208.
- [30] Ingólfssdottir K. In *Bioactive Carbohydrate Polymers*, Kluwer Academic Publishers: England, 2000, Vol. 44, p 25–36.
- [31] Box GEP, Hunter WG, Hunter JS. *Statistics for Experimenters*. John Wiley and Sons: New York, 1978, pp 291–334.
- [32] Montgomery DC. *Design and Analysis of Experiments*, 4th ed., John Wiley and Sons: New York, USA, 1996, pp 575–651.
- [33] Jiale H, Qingbiao L, Daohua S, Yinghua L, Yuanbo S, Xin Y. *Nanotechnology* 2007, 18, 105104–105115.
- [34] Fayaz AM, Balaji K, Kalaichelvan PT, Venkatesan R. *Colloids Surf., B* 2009, 74, 123–126.
- [35] Sathishkumar M, Sneha K, Won SW, Cho CW, Kim S, Yun YS. *Colloids Surf., B* 2009, 73, 332–338.
- [36] Sathiyarayanan G, Seghal Kiranb G, Joseph S. *Colloids Surf., B* 2013, 102, 13–20.
- [37] Janardhanan R, Karuppaiah M, Hebalkar N, Rao TN. *Polyhedron* 2009, 28, 2522–2530.
- [38] Philip D. *Spectrochim. Acta, Part A* 2010, 75, 1078–1081.
- [39] Bankar A, Joshi B, Kumar AR, Zinjarde S. *Colloids Surf., B* 2010, 80, 45–50.
- [40] Prakash P, Gnanaprakasam P, Emmanuel R, Arokiyaraj S, Saravanan M. *Colloids Surf., B* 2013, 108, 255–259.
- [41] Kumar DA, Palanichamy V, Roopan SM. *Spectrochim. Acta, Part A* 2014, 127, 168–171.
- [42] Sun Q, Cai X, Li J, Zheng M, Chen Z, Yu CP. *Colloids Surf., A* 2014, 444, 226–231.
- [43] Dong C, Zhang X, Cai H. *J. Alloys Compd.* 2014, 583, 267–271.



Nuray Yıldız is a Professor of Chemical Engineering at the University of Ankara. She obtained a PhD in Chemical Technologies in 1997 at Ankara University in Turkey. Her research interests include waste water treatment, synthesis of polymer, nanoparticles (RESS process), core-shell (magnetic nanoparticles-polymer) nanocomposites and also regeneration of adsorbents and extraction using supercritical fluids, synthesis of nanomaterials using plant extract and synthesis of graphene and its composites by green chemistry methods (supercritical fluids and biosynthesis). She has published numerous papers in the areas of materials science, waste water treatment, extraction, synthesis and characterization.



Çağlar Ateş obtained his undergraduate degree in Chemical Engineering at University of Ankara in 2011. During collegian, his research focused on synthesis of metal nanoparticles using the extracts of natural plants. He is currently working as a manufacturing engineer.



Mehmet Yılmaz received both his BS and MS in chemical engineering from Hacettepe University and Ankara University in 2005 and in 2009, respectively. He is pursuing his PhD in the Bioengineering Department at Hacettepe University. He is currently focused on the synthesis of functional nanomaterials and manufacture of nanopatterned surfaces, as well as their applications in sensing, therapy and bioimaging.



Dürdane Demir graduated from the University of Ankara with a degree in Chemical Engineering in 2012. As an undergraduate, her interest focused on biosynthesis of metal nanoparticles. She is currently working as an air traffic controller at Turkish Airlines.



Atila Yıldız is an Associate Professor at the Department of Biology, Ankara University. He obtained his PhD in Biology at Ankara University, Turkey. His research focuses on waste water treatment, heavy metals biomonitoring in the air, biosynthesis of metal nanoparticles, systematic botany and ecology.



Ayla Çalıklı is a Professor of Chemical Engineering at University of Ankara. She obtained her PhD in Chemical Technologies in 1978 at the Ankara University in Turkey. Her research interests include bioceramic materials, waste water treatment, synthesis of polymer, nanoparticles, scaffold materials and nanocomposites and also regeneration of adsorbates and extraction using supercritical fluids, synthesis of nanomaterials using plant extract and synthesis of carbon based composites by green chemistry methods. She has published numerous papers in the areas of materials science, waste water treatment, extraction and synthesis.